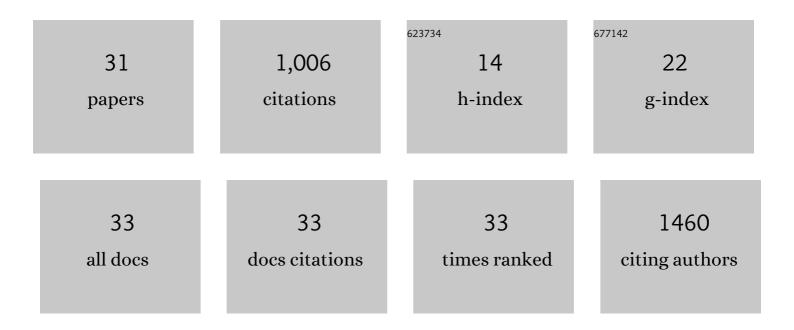
Muhammad Hasan Ali Baig

List of Publications by Year in descending order

Source: https://exaly.com/author-pdf/724184/publications.pdf Version: 2024-02-01



#	Article	IF	CITATIONS
1	Derivation of a tasselled cap transformation based on Landsat 8 at-satellite reflectance. Remote Sensing Letters, 2014, 5, 423-431.	1.4	462
2	Evaluation of Spatial and Temporal Performances of ERA-Interim Precipitation and Temperature in Mainland China. Journal of Climate, 2018, 31, 4347-4365.	3.2	87
3	Comparison of the Continuity of Vegetation Indices Derived from Landsat 8 OLI and Landsat 7 ETM+ Data among Different Vegetation Types. Remote Sensing, 2015, 7, 13485-13506.	4.0	50
4	A Simple Enhanced Water Index (EWI) for Percent Surface Water Estimation Using Landsat Data. IEEE Journal of Selected Topics in Applied Earth Observations and Remote Sensing, 2015, 8, 90-97.	4.9	48
5	Understanding long-term (1982–2013) patterns and trends in winter wheat spring green-up date over the North China Plain. International Journal of Applied Earth Observation and Geoinformation, 2017, 57, 235-244.	2.8	46
6	Mapping sugarcane in complex landscapes by integrating multi-temporal Sentinel-2 images and machine learning algorithms. Land Use Policy, 2019, 88, 104190.	5.6	44
7	Lake water surface mapping in the Tibetan Plateau using the MODIS MOD09Q1 product. Remote Sensing Letters, 2017, 8, 224-233.	1.4	38
8	Biophysical effect of conversion from croplands to grasslands in water-limited temperate regions of China. Science of the Total Environment, 2019, 648, 315-324.	8.0	28
9	Ensemble Learning with Multiple Classifiers and Polarimetric Features for Polarized SAR Image Classification. Photogrammetric Engineering and Remote Sensing, 2014, 80, 239-251.	0.6	26
10	Time series of the Inland Surface Water Dataset in China (ISWDC) for 2000–2016 derived from MODIS archives. Earth System Science Data, 2019, 11, 1099-1108.	9.9	24
11	Monitoring vegetation dynamics using the universal normalized vegetation index (UNVI): An optimized vegetation index-VIUPD. Remote Sensing Letters, 2019, 10, 629-638.	1.4	22
12	Large-Scale Surface Water Mapping Based on Landsat and Sentinel-1 Images. Water (Switzerland), 2022, 14, 1454.	2.7	22
13	Assessing Meteorological and Agricultural Drought in Chitral Kabul River Basin Using Multiple Drought Indices. Remote Sensing, 2020, 12, 1417.	4.0	20
14	COmparison of MNDWI and DFI for water mapping in flooding season. , 2013, , .		14
15	Estimating the area burned by agricultural fires from Landsat 8 Data using the Vegetation Difference Index and Burn Scar Index. International Journal of Wildland Fire, 2018, 27, 217.	2.4	14
16	Assessment of forest cover and carbon stock changes in sub-tropical pine forest of Azad Jammu & Kashmir (AJK), Pakistan using multi-temporal Landsat satellite data and field inventory. PLoS ONE, 2020, 15, e0226341.	2.5	12
17	Twenty-first century hydrologic and climatic changes over the scarcely gauged Jhelum river basin of Himalayan region using SDSM and RCPs. Environmental Science and Pollution Research, 2022, 29, 11196-11208.	5.3	10
18	Exploring the potential of Sentinel-2A satellite data for aboveground biomass estimation in fragmented Himalayan subtropical pine forest. Journal of Mountain Science, 2020, 17, 2880-2896.	2.0	8

#	Article	IF	CITATIONS
19	Line matching of wide baseline images in an affine projection space. International Journal of Remote Sensing, 2020, 41, 632-654.	2.9	7
20	Automated detection of coastline using Landsat TM based on water index and edge detection methods. , 2012, , .		4
21	Winter Wheat Take-All Disease Index Estimation Model Based on Hyperspectral Data. Applied Sciences (Switzerland), 2021, 11, 9230.	2.5	4
22	Patterns and causes of winter wheat and summer maize rotation area change over the North China Plain. Environmental Research Letters, 2022, 17, 044056.	5.2	4
23	Using MODTRAN4 to build up a general look-up-table database for the atmospheric correction of hyperspectral imagery. , 2012, , .		2
24	Hydrological ecosystem changes and impacts after the Zonag Lake outburst in Hoh Xil of Tibetan Plateau. Journal of Asian Earth Sciences: X, 2021, 6, 100064.	0.9	2
25	Framework for Monitoring the Spatiotemporal Distribution and Clustering of Drought Characteristics in Hunan Province. Applied Sciences (Switzerland), 2021, 11, 11524.	2.5	2
26	Calculating vegetation index based on the universal pattern decomposition method (VIUPD) using Landsat 8. , 2014, , .		1
27	Water mapping through Universal Pattern Decomposition Method and Tasseled Cap Transformation. , 2014, , .		1
28	WETLAND CHANGE DETECTION IN PROTECTED AND UNPROTECTED INDUS COASTAL AND INLAND DELTA. International Archives of the Photogrammetry, Remote Sensing and Spatial Information Sciences - ISPRS Archives, 0, XLII-2/W7, 1495-1501.	0.2	1
29	Mapping of debris-covered glaciers in Astor basin: an object-based image analysis approach. , 2018, , .		1
30	A preliminary study on the application of remotely sensed SST in locating evaporation duct height. Proceedings of SPIE, 2012, , .	0.8	0
31	Assessment of estimation methods for Chlorophyll-a through hyperspectral insitu data and multispectral landsat for Taihu lake. , 2013, , .		0